Abrupt Transition from a Free, Repulsive to a Condensed, Attractive DNA Phase, Induced by Multivalent Polyamine Cations

Xiangyun Qiu, Kurt Andresen, Jessica S. Lamb, Lisa W. Kwok, and Lois Pollack
School of Applied and Engineering Physics, Cornell University, Ithaca, New York 14853, USA
(Received 3 June 2008; published 26 November 2008)

We have investigated the energetics of DNA condensation by multivalent polyamine cations. Solution small angle x-ray scattering was used to monitor interactions between short 25 base pair dsDNA strands in the free supernatant DNA phase that coexists with the condensed DNA phase. Interestingly, when tetravalent spermine is used, significant inter-DNA repulsion is observed in the free phase, in contrast with the presumed inter-DNA attraction in the coexisting condensed phase. DNA condensation thus appears to be a discrete, first-order-like, transition from a repulsive gaseous to an attractive condensed solid phase, in accord with the reported all-or-none condensation of giant DNA. We further quantify the electrostatic repulsive potentials in the free DNA phase and estimate the number of additional spermine cations that bind to DNA upon condensation.

DOI: 10.1103/PhysRevLett.101.228101 PACS numbers: 87.14.gk, 87.15.nr, 87.15.rp, 87.15.Zg

DNA condensation is important to both biology and therapeutics, enabling the highly compact storage of genetic materials *in vivo* and DNA manipulations for gene therapy. Although interaction with proteins drives *in vivo* packaging, it is well known that small multivalent cations effectively condense highly negatively charged DNA *in vitro* [1]. Though a topic of active research for many years, the true physical origin of the intriguing attraction between like-charged DNAs is still unresolved.

A theoretical explanation of this effect clearly requires considerations beyond the mean field Poisson-Boltzmann treatment which always predicts like-charge repulsion [2]. Numerous theories have therefore evolved to explain this attraction. Consideration of counterion correlations suggests either density fluctuations distant from the surface [3] or ionic 2D ordering near the surface [4] can result in attraction. Consideration of the discreteness of the DNA charge shows that the *local* molecular fields lead to significant cation binding and such charge undulations can result in attraction [5,6]. The helical charge pattern of dsDNA inspired the proposed ''zipper mechanism'' by cation binding into the grooves rather than the charged groups [7]. Restructuring of the hydrated water by cations may result in attractive hydration forces, as concluded from extensive osmotic stress measurement [8]. While numerical simulations have confirmed inter-DNA attraction in the presence of multivalent cations, endorsing a particular theory proves difficult for such a complex system with multiple degrees of freedom [9]. This topic has been reviewed extensively [1,9,10].

Experimental studies have focused on characterizing the condensed DNA phase, precipitated by polycations such as cobalt^{3+} hexammine. CryoEM and x-ray diffraction measurements revealed that condensed DNA orders in hexagonal arrays [11,12] with side-by-side alignment. The inter-DNA spacing depends on the ion type, but is essentially constant from low to moderate multivalent ion concentrations [12,13]. High multivalent salt leads to gradual expansion and eventual redissolvation of the condensed DNA arrays [12,13]. To avoid the complication of non-negligible ion pairing in high salts [13], the work described here focuses on the dilute multivalent ion regime. The apparent inter-DNA attraction mediated by counterions is estimated to be weak, on the order of 0.1 kT per base pair (bp). The pioneering osmotic stress measurements of condensed DNA arrays by Rau and Parsegian [8] deduced an attractive free energy minimum of $\sim$0.17 kT/bp upon condensation in 20 mM cobalt hexammine 200 mM NaCl. Similar estimates have been derived from recent single molecule pulling experiments with optical and magnetic tweezers [14,15]. Despite significant progress due to recent intense experimental efforts [1], physical interpretations of the forces driving the condensation process are still tentative.

In contrast, little is known about how multivalent cations weaken the initial strong inter-DNA repulsion and induce the inter-DNA attraction that precedes precipitation. For example, it is known that the [spermine] to [DNA phosphate] ratio $r_{S/P}$ needs to reach $\sim$20% to *initiate* DNA precipitation (except in solutions with dilute DNA or high ionic strength) [12], but when and how does the attraction set in? In the two-phase coexistence regime that exists prior to complete DNA precipitation at $r_{S/P} \sim 25\%$ (i.e., total charge neutralization) [12], we have not yet learned the nature of DNA interaction in the coexisting supernatant free DNA phase.

Employing a well-defined system of short rigid rodlike dsDNA strands amenable to quantitative analysis, we characterized the free DNA phase using small angle x-ray scattering (SAXS). This method has been successfully applied to quantify inter-DNA pair potentials in semidilute solutions [16,17]. Surprisingly, for both counterions studied, spermidine^{3+} and spermine^{4+}, no signs of inter-DNA attraction were observed in the free DNA phase even in coexistence with the condensed DNA phase. Moreover,

significant inter-DNA repulsion persists in the case of spermine^{4+}, indicating the coexistence of free, repulsive and condensed, attractive DNA phases.

Single strand 25 base DNA oligos were purchased from IDT. Complementary strands were annealed at equimolar concentrations in *p*H 7 sodium 3-(N-morpholino) propanesulfonic acid (MOPS) buffered NaCl salt. Spermidine and spermine chloride salts were from Sigma. As SAXS measurements require relatively concentrated DNA solutions (>0.1 mM, 1.5 mg/ml), direct use of this DNA stock will result in elevated monovalent salt content, and may significantly complicate SAXS data analysis. We reduced the monovalent salt level by dialyzing against *limited* volumes of dilute multivalent salt buffer, as complete dialysis against even very low multivalent buffer will lead to substantial DNA precipitation. The new stock was then used to mix with appropriate amount of multivalent salt to give the nominal salt concentrations. For each sample, the residual [Na^+] (between 5 and 16 mM; see Ref. [18] for details about the sample preparation and concentration analysis) was measured by atomic emission spectroscopy at Cornell Nutrient Analysis Laboratories; [Cl^-] was verified as the nominal value by ion chromatography by the Soil and Plant Analysis Lab at University of Wisconsin. DNA concentrations were given by the [phosphorus]s from atomic emission spectroscopy and verified by uv absorption at 260 nm. Solution SAXS measurements were carried out at the G1 station of the Cornell High Energy Synchrotron Source (CHESS). The x-ray exposure time was selected to avoid radiation damage (scattering profiles were time independent).

Above a certain threshold, adding more multivalent polyamine cations leads to instantaneous clouding and precipitation of DNA strands, and results in two coexisting DNA phases: the free DNA strands in the supernatant and the condensed DNA precipitates. The amount of precipitated DNA grows with further addition of polyamine ions. Correspondingly, the concentration of free DNAs in solution decreases, as shown in Fig. 1, where the shaded area indicates the presence of visible precipitates (from the third point for both spermidine and spermine). At very high polyamine concentrations, the redissolvation of precipitated DNA strands leads to an increase in the measured free DNA concentration.

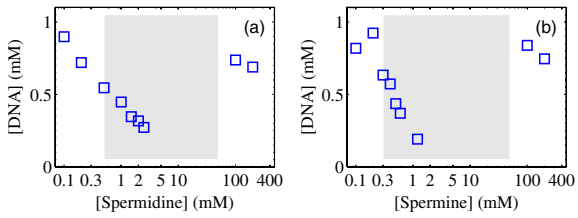

FIG. 1 (color online). The [DNA] in the supernatant as a function of nominal [spermidine] (a) or [spermine] (b). Note that [phosphate] = 48 × [DNA]. Shaded areas indicate the presence of precipitates. Variations of the first two points result from different dilutions when mixing up sample solutions.

We first characterized the condensed DNA phase for these short duplexes, as earlier studies were carried out on much longer strands [8,12]. We used polarization microscopy to confirm the liquid crystalline nature and carried out x-ray diffraction measurements to verify the hexagonal packing of DNA arrays. Condensed DNA phases in this study show a constant inter-DNA spacing (e.g., 28.23 Å for spermine), consistent with previously published results [8,12] (see Ref. [18] for more details on the spermine-DNA system). It is worth noting that the recently reported liquid crystal formation from short dsDNA [19] is due to very high oligomer concentration, while the origin of the liquid crystal phase observed here is most likely the counterion induced attraction.

SAXS measurements of semidilute macromolecular solutions report the nature of interparticle interactions. The measured scattering intensity $I(Q)$ ($Q = \frac{4\pi}{\lambda}\sin\theta$, λ is the x-ray wavelength, and 2θ is the scattering angle) has two components: the form factor $P(Q)$ of a single DNA, and the structure factor $S(Q)$. The inter-DNA interference function $S(Q)$ arises from long-range structural correlations, modulates the SAXS profile, and is most pronounced at low Q [20]. Figure 2 shows solution SAXS profiles of selected samples. In the single phase regime before the onset of the DNA precipitation, the corresponding SAXS profiles (the first two curves of each series) show very pronounced low Q downturns, evidence of strong inter-DNA repulsion [16]. Clearly, the repulsion weakens upon adding multivalent counterions, as expected from increased electrostatic screening.

For the spermine series [Fig. 2(b)], it is striking that the low Q downturn (i.e., inter-DNA repulsion) persists into the two-phase coexistence regime when the nominal [spermine] is greater than 0.3 mM. Note that only the supernatant DNA solution was loaded to the SAXS cell. This is surprising, as the coexisting condensed DNA phase requires a strong inter-DNA attraction. In contrast to our observation, attraction (i.e., a low Q upturn [17,21]) had

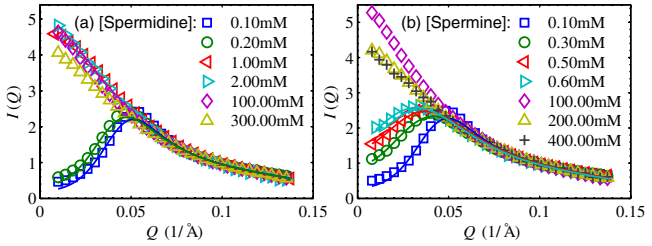

FIG. 2 (color online). Solution SAXS data of the supernatant DNA phase only in (a) spermidine and (b) spermine. Data (symbols) are scaled to match at high Q for easy comparison, and the lines are the fits. The lowering down of the low Q scattering intensity at highest salt concentrations (>100 mM) interpreted as from lower DNA contrast due to the increased solvent electron density (particularly high [Cl^-]).

naively been expected within the coexisting free DNA phase. The data, however, indicate the coexisting regime is composed of one repulsive gaseous phase and one attractive condensed solid phase. As no centrifugation was applied, our data ruled out the existence of microscopic DNA "clusters" before precipitation, as clusters will give a sharp low Q upturn [17]. DNA condensation by spermine appears to be an abrupt, first-order transition (discontinuous volume change).

Data acquired in the presence of the less highly charged polyamine, spermidine, exhibit less pronounced trends [Fig. 2(a)]. In the two-phase coexistence regime, the SAXS profiles resemble the scattering from individual (i.e., noninteracting) DNAs. However, no attractive force is measured (i.e., no low Q upturn). The difference can be rationalized as follows: the inter-DNA repulsion needs to be almost completely suppressed for spermidine to precipitate DNA strands, while spermine is capable of precipitating significantly repulsive DNA strands, consistent with the stronger condensing "power" of spermine. Note only weak inter-DNA attraction, consistent with end to end stacking and not with precipitation, was observed with Mg^{2+} [17]. In the redissolvation regime ([spermine] or [spermidine] $>$ 100 mM), DNA strands appear to interact weakly, and do not show clustering peaks.

More quantitative information can be extracted from analysis of the structure factor $S(Q)$. The generalized one-component method was used [22,23] to extract inter-DNA interactions in the form of a Yukawa-like pair potential plus a hard-core repulsion. The polyelectrolyte charge obtained from this analysis, the so-called renormalized effective charge Z_{eff}, is smaller than the bare charge due to the nonlinear screening by counterions. Details of the data analysis can be found in Ref. [16]. While the so-called "free" bulk (not total) ion concentrations are required to calculate ionic strengths, we obtained such values by iteratively solving the nonlinear Poisson-Boltzmann equations based on a cell model to match the total concentration of each constituent ion that was experimentally measured. We note that the dilute free multivalent ions contribute little to the ionic strength and our results are robust against such numerical treatments. Figure 3 shows that the effective charge Z_{eff} of DNA quickly decreases upon the initial addition of polyamine cations. Notably, considerably larger $[Na^+]$ ($\sim$100 mM) and $[Mg^{2+}]$ ($\sim$2 mM) are required to achieve the levels of screening by $\sim$0.3 mM spermidine or spermine [16,17]. Interestingly, in the two-phase coexistence regime, Z_{eff} remains essentially constant. While DNA appears to be completely neutralized by spermidine, DNA remains significantly charged in the presence of spermine ($\sim 6.0e$), reflecting differences in "condensing power."

With the free DNA phase well characterized, its thermodynamics can be calculated. Since such quantitative analysis is more accurate for strongly interacting molecules, we apply this treatment to the spermine series only. With the known inter-DNA pair potential $\phi(r)$ and DNA-

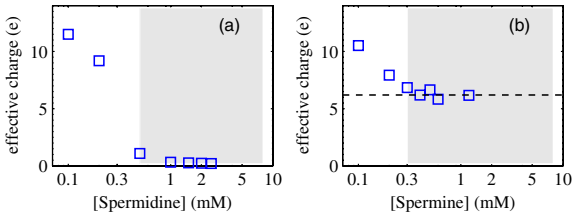

FIG. 3 (color online). Effective charge Z_{eff} of the free DNA strands in solution as a function of the nominal spermidine (a) or spermine (b) concentrations. Dashed line is a guide to the eye. Error bars are slightly smaller than symbol sizes.

DNA pair distribution function $g(r)$, we can compute the electrostatic potential energy Φ per DNA strand in the free solution phase according to

$$\Phi = 2\pi\rho \int_0^\infty \phi(r) g(r) r^2 dr, \tag{1}$$

where ρ is the number density of DNA strands. Note that Φ is independent of the hard-core regime where $g(r) = 0$. The potential energy Φ per DNA shown in Fig. 4(a) decreases monotonically, as expected from decreasing effective charge and/or decreasing DNA concentration. It is also straightforward to calculate the free energy G of DNA, or chemical potential, given $G = U + PV - TS$, where P is the osmotic pressure of DNA strands, and

$$PV/N = 1 - \frac{2}{3}\pi\rho \int_0^\infty \phi(r)' g(r) r^3 dr. \tag{2}$$

As the entropy of DNA in the condensed phase is unknown and it is required for absolute comparisons, we choose to ignore the unchanging components of the DNA entropy in the free DNA phase (e.g., the rotational entropy of DNA). We thus only consider the translational entropy of DNA as $-k\ln(c)$ (c is the DNA concentration). Thus only the relative values of the free energy G shown in Fig. 4(b) are meaningful.

Figure 4(b) shows that the free energy per DNA decreases by nearly 3.3 kT across the phase coexistence regime ($0.3 <$ [spermine] < 1.2 mM). However, for the coexisting condensed DNA phase throughout this regime, its inter-DNA spacing does not change; addition of spermine just brings more strands to the precipitate; a constant free energy is thus expected [12]. Phase equilibrium dic-

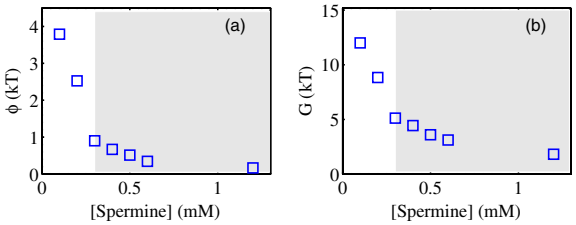

FIG. 4 (color online). Spermine series only. (a) Electrostatic potential energy Φ per DNA. (b) Free energy G per DNA with an offset.

tates that the free DNA phase should also have constant free energy, making the observed ~3.3 kT decrease rather disconcerting. This brings up one non-negligible event upon DNA condensation: additional counterion binding. Todd and Rau recently showed that the attractive energy is expended largely, if not all, to pay for the entropic loss of such counterions when condensing a single long DNA molecule [14]. To estimate the apparent number n of the additionally bound counterions, we assume n does not change across the phase coexisting regime where the same effective DNA charges are observed (Fig. 3). As the nominal [spermine] increases from 0.3 to 1.2 mM, our numerical procedure gives an increase of free [spermine] from 0.18 to 0.88 mM; i.e., the free energy of one spermine ion increases by $\ln(0.88/0.18) \sim 1.6$ kT. Thus, to make up the 3.3 kT decrease in DNA free energy, an additional binding of $n = 2.1$ spermine per DNA (~ 0.09/bp) is required, which is within the range known only for trivalent cations [14]. Given the relative low effective [spermine] (<1 mM) probed here, it is important to note that counterion binding alone is relevant, rather than release at higher [spermine] [14,15]. The implied 82% charge neutralization is also close to the ~80% neutralization before condensation for spermine in the literature [24].

We have adopted a well-defined system to quantitatively probe the energetics of free DNA phases that precede or coexist with the counterion precipitated DNA phase. The observed significant inter-DNA repulsion suggests that spermine induced DNA condensation occurs as an abrupt transition from a repulsive, free gaseous to an attractive, condensed solid phase. An energetic barrier is suggested from the first-order nature of the phase transition. Our results show that such a barrier is both electrostatic and entropic for spermine, while mostly entropic for spermidine. The sudden onset of attraction may reflect the requirement of cooperative rearrangement of counterions as DNA strands approach each other, while the rigidity of DNA may also be significant comparing to flexible polymers that can be condensed into a ''gel-like'' phase [6]. Moreover, our measurements were able to quantify the residual long-range electrostatic repulsion in the supernatant DNA phase, and show for the first time that a rather large effective charge persists in the presence of spermine. The short rigid oligomeric system enables quantitative analysis to test future theoretical developments, and provides unique insight into the energetics of DNA condensation.

Our observation of the abrupt two-state transition from repulsive to attractive DNA provides a physical explanation for various experimental observations in the literature. Yushikawa *et al.* extensively examined counterion induced collapse of a single long DNA [25,26], and observed a discrete size decrease between random coil and compact globule states. The sudden collapse of DNA arrays under increasing osmotic stress [8] also indicated a first-order transition. Pulling a single λ DNA with optical tweezers resulted in a force plateau, consistent with a distinct two-state transition [14,15].

The capacity of charged molecules as sensitive ionic switches between conformational states of DNA strands may carry biological and clinical implications, such as modulating chromatin structure for DNA access or repair or the packaging and release of therapeutic genes.

We thank Arthur Woll and Peter Busch for experimental assistance, Y. Liu and S.-H. Chen for their MATLAB codes, D. C. Rau and V. A. Parsegian for discussions. This research is funded by NIH, NSF, and the NBTC at Cornell. CHESS is supported by NSF and NIH/NIGMS.

[1] W. Gelbart, R. Bruinsma, P. Pincus, and V. Parsegian, Phys. Today **53**, No. 9, 38 (2000); F. Solis and M. O. de la Cruz, Phys. Today **54**, No. 1, 71 (2001); V. A. Bloomfield, Biopolymers **44**, 269 (1997).
[2] E. J. W. Verwey and J. T. G. Overbeek, *Theory of the Stability of Lyophobic Colloids* (Elsevier, New York, 1948).
[3] R. Kjellander and S. Marcelja, Chem. Phys. Lett. **112**, 49 (1984).
[4] I. Rouzina and V. A. Bloomfield, J. Phys. Chem. **100**, 9977 (1996); B. Shklovskii, Phys. Rev. Lett. **82**, 3268 (1999).
[5] A. Travesset and D. Vaknin, Europhys. Lett. **74**, 181 (2006); Z. Tan and S. Chen, Biophys. J. **91**, 518 (2006).
[6] M. O. de la Cruz *et al.*, J. Chem. Phys. **103**, 5781 (1995).
[7] A. Kornyshev and S. Leikin, Phys. Rev. Lett. **82**, 4138 (1999).
[8] D. C. Rau and V. A. Parsegian, Biophys. J. **61**, 246 (1992).
[9] H. Boroudjerdi *et al.*, Phys. Rep. **416**, 129 (2005).
[10] G. Wong, Curr. Opin. Colloid Interface Sci. **11**, 310 (2006).
[11] N. V. Hud and K. H. Downing, Proc. Natl. Acad. Sci. U.S.A. **98**, 14 925 (2001).
[12] E. Raspaud, D. Durand, and F. Livolant, Biophys. J. **88**, 392 (2005).
[13] J. Yang and D. Rau, Biophys. J. **89**, 1932 (2005).
[14] B. A. Todd and D. C. Rau, Nucleic Acids Res. **36**, 501 (2007).
[15] F. Ritort *et al.*, Phys. Rev. Lett. **96**, 118301 (2006); K. Besteman, K. Van Eijk, and S. G. Lemay, Nature Phys. **3**, 641 (2007); C. G. Baumann *et al.*, Proc. Natl. Acad. Sci. U.S.A. **94**, 6185 (1997).
[16] X. Qiu *et al.*, Phys. Rev. Lett. **96**, 138101 (2006).
[17] X. Qiu *et al.*, Phys. Rev. Lett. **99**, 038104 (2007).
[18] See EPAPS Document No. E-PRLTAO-101-025847 for supplemental data. For more information on EPAPS, see http://www.aip.org/pubservs/epaps.html.
[19] M. Nakata *et al.*, Science **318**, 1276 (2007).
[20] M. Koch *et al.*, Q. Rev. Biophys. **36**, 147 (2003).
[21] K. Andresen *et al.*, Biophys. J. **95**, 287 (2008).
[22] J. B. Hayter and J. Penfold, Mol. Phys. **42**, 109 (1981).
[23] S. H. Chen *et al.*, J. Appl. Crystallogr. **21**, 751 (1988).
[24] Y. Burak, G. Ariel, and D. Andelman, Biophys. J. **85**, 2100 (2003).
[25] K. Yoshikawa *et al.*, Phys. Rev. Lett. **76**, 3029 (1996).
[26] M. Takahashi *et al.*, J. Phys. Chem. B **101**, 9396 (1997).